

# 000 001 002 003 004 005 006 007 008 009 010 011 012 013 014 015 016 017 018 019 020 021 022 023 024 025 026 027 028 029 030 031 032 033 034 035 036 037 038 039 040 041 042 043 044 045 046 CONTAMINATION DETECTION FOR VLMs USING MULTI-MODAL SEMANTIC PERTURBATIONS

Anonymous authors

Paper under double-blind review

## ABSTRACT

Recent advances in Vision-Language Models (VLMs) have achieved state-of-the-art performance on numerous benchmark tasks. However, the use of internet-scale, often proprietary, pretraining corpora raises a critical concern for both practitioners and users: inflated performance due to *test-set leakage*. While prior work has proposed mitigation strategies such as decontamination of pretraining data and benchmark redesign for LLMs, the complementary direction of developing detection methods for *contaminated VLMs* remains underexplored. To address this gap, we deliberately contaminate open-source VLMs on popular benchmarks and show that existing detection approaches either fail outright or exhibit inconsistent behavior. We then propose a novel simple yet effective detection method based on *multi-modal semantic perturbation*, demonstrating that contaminated models fail to generalize under controlled perturbations. Finally, we validate our approach across multiple contamination strategies, confirming its robustness and effectiveness. The code and perturbed dataset will be released publicly.

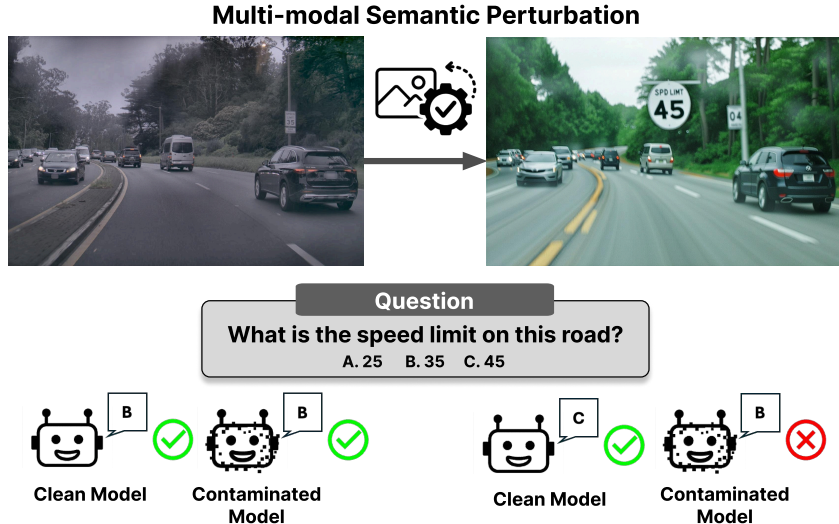


Figure 1: Example of our multi-modal semantic perturbation pipeline applied to RealWorldQA benchmark. Using ControlNet trained with Flux models, a new speed limit sign is generated, changing the correct answer from (B) to (C) while preserving the original image's overall composition. A contaminated model that has memorized the original question is likely to fail on the perturbed version.

## 1 INTRODUCTION

Recent advances in Vision-Language Models (VLMs) have achieved remarkable performance across a wide range of tasks, including visual reasoning (Yue et al., 2024; Liu et al., 2024b; Chen et al., 2024a), real-world understanding (xAI, 2024), and complex mathematical problems (Zhang et al., 2024b; Lu et al., 2024b). A typical VLM training pipeline involves pretraining a vision encoder and language backbone on internet-scale data, followed by fine-tuning on high-quality multimodal instruction-tuning datasets. However, as these training corpora are often proprietary with their exact

Requirements		Reliability	Practicality	Consistency
N-gram Accuracy	(Xu et al., 2024)	✗	✗	✗
Shared Likelihood	(Oren et al., 2023)	✗	✗	✗
Guided Prompting	(Golchin & Surdeanu, 2024)	✗	✗	✗
Multi-modal Leakage	(Chen et al., 2024a)	✗	✗	▲
CircularEval	(Liu et al., 2024b)	▲	✗	✗
Choice Confusion	(Yao et al., 2024)	✗	✓	▲
BGR Shuffling	(Lu et al., 2024a)	✗	✗	✗
Image Masking / Option Shuffling	(Song et al., 2025)	✗	✗	✗
Multi-modal Semantic Perturbation	<b>Ours</b>	✓	✓	✓

Table 1: Analysis of existing detection methods on VLMs. We label the detection method with ✓ if it satisfies all of Requirement 1, 2 or 3 and with ✗ otherwise. ▲ indicates that the requirement is partially observed but not consistently with varying contamination settings. Most existing detection methods fail to meet the requirements and cannot accurately classify contaminated models. Our method, however, satisfies all requirements. Detailed results and analysis is included in the Appendix.

composition undisclosed, a critical concern has emerged: the potential for public benchmark data to have leaked into the training set, leading to inflated and misleading performance metrics.

Test-set leakage presents a practical and significant challenge. For model users, it becomes difficult to disentangle genuine reasoning and generalization from mere memorization. For developers, exhaustively verifying the absence of test examples in massive pretraining corpora is prohibitively expensive. Although early work on large models proposed decontamination steps by removing n-gram overlaps (Brown et al., 2020; Bai et al., 2023; Abdin et al., 2024a), many recent models do not report such procedures, leaving the extent of contamination largely unexamined.

To address this, several methods have been proposed to detect data contamination. One line of work focuses on *verbatim memorization*, testing whether a model can reconstruct exact benchmark questions with high confidence (Xu et al., 2024; Golchin & Surdeanu, 2024; Oren et al., 2023). Another line of work examines *generalization failures*, measuring if a model that succeeds on an original question fails on a simpler variant, which is interpreted as evidence of memorization (Mirzadeh et al., 2024; Yao et al., 2024; Huang et al., 2025).

However, these detection methods were primarily designed for Large Language Models (LLMs) and often overlook the unique, multi-modal nature of VLMs. Applying simple text-based perturbations to a VLM may not be sufficient, as the model could rely on visual features that remain unchanged. This discrepancy exposes a critical gap and raises a key question:

*Is there a reliable, practical, and consistent method for detecting contamination in VLMs?*

In this study, we conduct a systematic analysis of the data contamination problem, from which we derive grounded definitions of the core requirements – reliability, practicality, and consistency. Guided by these definitions, we systematically contaminate open-source VLMs under varying fine-tuning epochs, data composition, and training strategies (e.g., standard fine-tuning vs. LoRA (Hu et al., 2021)). Our results show that existing detection methods struggle with the complexities of VLMs, frequently failing to meet the core requirements across diverse contamination scenarios (see Table 1).

To overcome these limitations, we introduce a novel **multi-modal semantic perturbation** pipeline. Our method generates new test examples by subtly altering the semantics of the *image* while preserving its overall composition, thereby creating variants of comparable or lower difficulty (Figure 1). The core principle is that a contaminated model, which has merely memorized an image-text pair, will fail to generalize to this perturbed input. In contrast, a clean model with genuine reasoning capabilities should perform correctly. This approach enables robust contamination detection without requiring any ground-truth knowledge of the leaked data.

108 Our contributions are threefold:  
 109

- 110 We propose a novel, simple yet effective detection framework based on multi-modal semantic  
 111 perturbations, which effectively identifies contaminated models by testing for generalization  
 112 failures in the visual domain.
- 113 We validate our method across multiple contamination settings, proving that it is reliable,  
 114 practical, and consistent, satisfying all key requirements for a robust detection method.
- 115 We conduct the first systematic study of VLM behavior under diverse contamination and  
 116 detection strategies, demonstrating that existing methods designed for LLMs are often unreliable  
 117 for VLMs.

118 **2 INVESTIGATION SETUP**  
 119

120 This section establishes the formal framework for our analysis of data contamination. We begin by  
 121 defining the degree of contamination, state our core assumption about its relationship with model  
 122 generalization, and finally, outline three essential requirements for a robust detection method.  
 123

124 Our analysis is built upon a formal definition of contamination at the data-point level. For a given  
 125 data point  $x$ , a contamination dataset  $\mathcal{D}$ , and a training process consisting of  $n$  epochs, we define:

126 **Definition 1.** (Degree of Contamination). The *degree of contamination* for a data point  $x$  is:  
 127

$$128 \quad \text{deg}(x) = \left( \sum_{d \in \mathcal{D}} \mathbf{1}_{\{x=d\}} \right) \times n.$$

131 This quantity reflects the total number of times  $x$  is seen during training. In our experimental  
 132 setup, where a model  $\mathcal{M}$  is fine-tuned on the entire benchmark dataset  $\mathcal{D}$  for  $n$  epochs, this  
 133 simplifies to  $\text{deg}(\mathcal{M}) = n$ .  
 134

135 This definition motivates our central assumption, grounded in prior work on model memorization  
 136 (Zhang et al., 2017; Carlini et al., 2021; Kandpal et al., 2023):

137 **Assumption 1.** Data points with a higher degree of contamination are more likely to be memo-  
 138 rized, which increases overfitting risk and impairs generalization.  
 139

140 In particular, we posit that as the degree of contamination grows, models will exhibit degraded  
 141 performance on perturbed or out-of-distribution variants of benchmark items, even when the orig-  
 142 inal questions are answered correctly. The effect need not scale linearly, since fine-tuning can  
 143 disproportionately distort embedding spaces (Choi et al., 2025).

144 Based on Assumption 1, we argue that any practical and effective detection method must satisfy three  
 145 fundamental requirements:

147 **Requirement 1.** (Practicality). The method must operate without the knowledge of the leaked  
 148 data or the model’s training corpus, relying only on black-box interactions.

149 **Requirement 2.** (Reliability). The method must detect contaminated models across heteroge-  
 150 neous fine-tuning strategies (e.g., standard fine-tuning vs. LoRA).

152 **Requirement 3.** (Consistency). The method’s detection signal should be positively correlated  
 153 with degree of contamination (i.e.,  $n = \text{deg}(\mathcal{D})$ ).  
 154

155 Together, these requirements define a principled framework for evaluating contamination detection.  
 156 A method that satisfies all of them can reliably flag contaminated models, remain agnostic to training  
 157 specifics, and provide a signal proportional to the extent of contamination.

158 **3 PREPARATION OF CONTAMINATED MODELS**  
 159

161 **Models and Benchmarks.** To analyze contamination detection across diverse settings, we pair com-  
 162 plementary model families and benchmarks. On the model side, we use LLaVA-v1.5-7B (Liu et al.,

2024a) – a LLaMA–adapter design – and Qwen2-VL-7B (Wang et al., 2024), which integrates tighter  
 163 multimodal alignment. Both are widely adopted open-source VLMs with publicly documented training  
 164 details (e.g., released corpora or decontamination policies), making them suitable for controlled  
 165 contamination experiments. Spanning these distinct training paradigms lets us probe robustness under  
 166 heterogeneous contamination footprints.

167 For benchmarks, we use MMStar (Chen et al., 2024a) and RealWorldQA (xAI, 2024), which both  
 168 require visual *and* textual evidence. MMStar aggregates and filters prior tasks to remove leaked or  
 169 non-visual items, while RealWorldQA enforces visual dependence by design. This prevents linguistic  
 170 shortcuts and ensures our perturbation-based detector evaluates genuine vision–language reasoning.

171 **Training Strategies.** We contaminate models by training directly on evaluation data. Because VLM  
 172 training typically has two stages—(i) large-scale pretraining of the vision encoder and language back-  
 173 bone and (ii) instruction-tuned multimodal fine-tuning—leakage can arise at either stage. Ablating  
 174 pretraining is computationally prohibitive, so we focus on *continual fine-tuning*, which affords precise  
 175 control over contamination levels.

176 We compare standard fine-tuning and LoRA (Hu et al., 2021). For standard fine-tuning, we follow  
 177 three common variants: fine-tune the LLM and adapter as in LLaVA-v1.5-7B; fine-tune only the  
 178 LLM as in Qwen2-VL-7B; or unfreeze all parameters as in InternVL (Chen et al., 2024b). This  
 179 diversity tests robustness across parameter-efficient and full fine-tuning regimes.

180 **Epochs.** We save checkpoints at epochs 1–3 (i.e.  $\deg(\mathcal{M}) \in \{1, 2, 3\}$ ), since VLMs are typically  
 181 fine-tuned for at most three epochs – and often just one. Contamination footprints of varying strength  
 182 enables a graded analysis of detection sensitivity (Liu et al., 2024a; Chen et al., 2025).

183 **Hyperparameters.** We use model defaults, adjusting only the learning rate to inflate test performance.  
 184 For LLaVA-v1.5-7B, we follow the official repo; for Qwen2-VL-7B, we use LLaMA-  
 185 Factory (Zheng et al., 2024). (Full settings are in the Appendix A.1.)

## 187 4 MULTI-MODAL SEMANTIC PERTURBATION

189 We propose multi-modal semantic perturbation framework for contamination detection, that generates  
 190 variants of image–text pairs with modified answers while keeping the original image composition  
 191 intact. In controlled experiments, our method consistently detects contaminated models and satisfies  
 192 all three requirements, while existing methods fail to yield a stable signal of test-set leakage in VLMs.

193 To generate semantically perturbed questions, we combine an LLM with a diffusion-based generative  
 194 model. In our main experiments, we use GPT-4o (OpenAI, 2024) and Flux (Labs, 2024) + ControlNet  
 195 (Zhang et al., 2023), but later show that our framework is model-agnostic through ablation studies.

197 The pipeline of our framework is as follows. First, we randomly **change the answer of the original**  
 198 **question** to a different option, preventing contaminated models from getting away with memorized  
 199 responses. Next, GPT-4o generates a dense caption of the image, conditioned both on the original  
 200 question, original answer and the newly chosen answer choice. We find this explicit conditioning  
 201 essential: it ensures the caption highlights the salient visual features required to answer the question  
 202 (Section 6). Flux ControlNet then uses this caption, together with Canny edge maps (Canny, 1986), to  
 203 guide the diffusion process. ControlNet preserves the global structure of the image while introducing  
 204 new elements that *minimally* alter semantics, yielding an updated image with a different correct  
 205 answer (Figure 2). We note that, due to limitations in rendering text or complex geometries, especially  
 206 at low resolution, some generated images do not fully correspond to the new answer. To mitigate  
 207 this, we filter generated pairs using a single criterion: perturbed questions must be answerable  
 208 unambiguously.<sup>1</sup> For the main results, we apply manual filtering to demonstrate the upper-bound  
 209 performance of our approach. However, as shown in Table 9, this manual step can be replaced with  
 210 automated filtering with a strong reasoning model.

210 **To detect whether a model is contaminated on a dataset-level, i.e. has memorized the training**  
 211 **image–text pairs, we compare its aggregate performance (i.e. accuracy) on the original vs. perturbed**  
 212 **benchmarks. If the model fails to generalize (i.e. it gets the original input correct but the perturbed one**

213 <sup>1</sup>Generation quality itself is not considered. This ensures that the evaluation set focuses solely on reasoning  
 214 rather than visual fidelity. While our main results report human-filtered outcomes, we show in Table 9 that this  
 215 step can be automated. We stress that filtering is necessitated by current generative model limitations, not by our  
 216 detection principle.

incorrect, leading to a lower performance on the perturbed benchmark), we flag contamination<sup>2</sup>. This is because a clean model with genuine reasoning capabilities should perform correctly in both settings, given that they have comparable difficulty. Critically, our approach enables robust contamination detection without requiring any ground-truth knowledge of the leaked data.

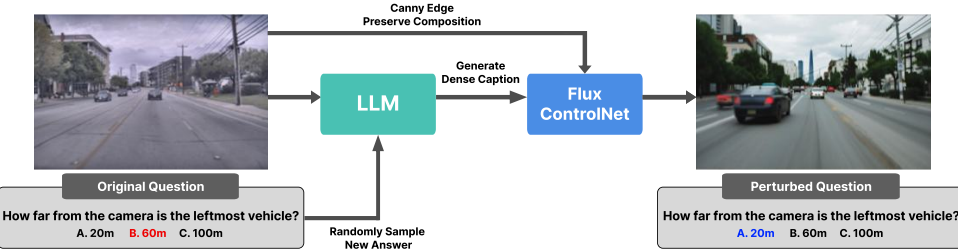


Figure 2: Illustration of our multi-modal semantic perturbation pipeline. The original question–image pair is used to generate a dense caption with an LLM, which guides Flux ControlNet to produce a perturbed image and new answer, yielding a modified but semantically consistent benchmark sample.

## 5 COMPARATIVE EVALUATION OF CONTAMINATION DETECTION

In this section, we present our main results: [detecting contamination on a dataset level](#). After perturbation and filtering, 440 image–question pairs remain from the original 765 in RealWorldQA, and 478 remain from 1,500 in MMStar (Section 6 shows that these are representative subsets). Table 2 reports results for MMStar; results for RealWorldQA are in the Appendix (Table 12).

First, we see that clean models perform better than contaminated models, confirming that the perturbed questions are indeed of equal or lower difficulty. In contrast, *all* contaminated models perform worse, enabling our method to reliably detect via a simple check for performance drops.

We compare to the following contamination detection methods:

**Multi-modal Leakage** (Chen et al., 2024a). With multi-modal leakage, contamination is flagged by measuring text-only performance on benchmarks that require visual input. After fine-tuning, any boost in text-only performance indicates memorization of leaked question–answer pairs rather than genuine multi-modal reasoning. Multi-modal leakage requires clean models by design and hence does not satisfy Practicality (Req. 1). And from Table 2 we observe that Reliability (Req. 2) is not satisfied since it fails to detect LLaVA-v1.5-7B trained for 3 epochs with standard fine-tuning. While its gain in performance positively correlates with the degree of contamination in other cases, this trend breaks across benchmarks and training strategies such as for Qwen2-VL-7B trained for 3 epochs with LoRA and LLaVA-v1.5-7B trained for 3 epochs with standard fine-tuning, thus only partially satisfying Consistency (Req. 3).

**CircularEval** (Liu et al., 2024b). Selection bias in multiple-choice questions is mitigated by rotating answer options  $n$  times and requiring the model to be correct on all rotations. This stricter criterion lowers absolute accuracy compared to standard evaluation. For contamination detection, however, CircularEval’s effectiveness is limited. Practicality (Req. 1) fails, as CircularEval lacks a clear threshold-independent detection mechanism. Reliability (Req. 2) is undermined by inconsistent contamination signals, as it fails to detect LLaVA-v1.5-7B trained with LoRA for 2 and 3 epochs, and Qwen2-VL-7B trained with standard fine-tuning for 2 epochs. And despite some positive trends, Consistency (Req. 3) breaks across models and training setups, as shown with LLaVA-v1.5-7B trained with LoRA for 2, 3 epochs and Qwen2-VL-7B trained with standard fine-tuning for 2, 3 epochs, limiting its diagnostic value.

**Choice confusion** (Yao et al., 2024). Generalization is tested by constructing an easier benchmark variant: false options are replaced with correct answers drawn from unrelated questions. Clean models should leverage this simplification to improve, whereas contaminated models—bound by memorized original answers—might not. We apply this method to measure the model’s performance drop ( $\Delta$ )

<sup>2</sup>We make a note that our approach can also be used to detect contamination on a **sample-level** by comparing the model’s behavior on the perturbed sample instead of the aggregate performance.

270 271	Method	Metric	LLaVA-v1.5-7B (clean)		LoRA (contaminated)			LLM+MLP (contaminated)			Require clean model? (Practicality (Req. 1))	
			—	Epoch 1	Epoch 2	Epoch 3	Epoch 1	Epoch 2	Epoch 3			
272 273 274	Ours	MMStar	37.78	52.53	50.71	54.34	41.82	48.89	50.71	No ✓		
		MMStar_P	69.29	44.24	37.58	38.18	33.33	37.37	36.97			
		Δ	+31.51	-8.29	-13.13	-16.16	-8.49	-11.52	-13.74			
		Success?	✓	✓	✓	✓	✓	✓	✓			
275 276 277	CircularEval	MMStar	37.78	52.53	50.71	54.34	41.82	48.89	50.71	Yes ✗		
		MMStar_C	26.06	29.09	45.66	55.56	25.86	22.83	22.02			
		Δ	-11.72	-23.44	-5.05	+1.22	-15.96	-26.06	-28.69			
		Success?	—	✓	✗	✗	✓	✓	✓			
278 279 280	Choice Confusion	MMStar	37.78	52.53	50.71	54.34	41.82	48.89	50.71	No ✓		
		MMStar_G	71.92	53.54	65.66	69.09	62.83	66.26	62.83			
		Δ	+34.14	+1.01	+14.95	+14.75	+21.01	+17.37	+12.12			
		Success?	✓	✗	✗	✗	✗	✗	✗			
281 282 283	Multi-modal Leakage	MMStar_to	19.39	26.67	29.70	30.51	19.80	26.87	8.69	Yes ✗		
		Δ	—	+7.28	+10.31	+11.12	+0.41	+7.48	-10.70			
		Success?	—	✓	✓	✓	✓	✓	✓			
		Success?	—	✓	✓	✓	✓	✓	✗			
284 285	Method	Metric	Qwen2-VL-7B (clean)		LoRA (contaminated)			LLM only (contaminated)			Require clean model? (Practicality (Req. 1))	
			—	Epoch 1	Epoch 2	Epoch 3	Epoch 1	Epoch 2	Epoch 3			
286 287 288	Ours	MMStar	62.02	78.38	94.14	95.96	89.90	97.98	98.99	No ✓		
		MMStar_P	78.18	71.31	65.25	63.64	60.40	54.95	55.96			
		Δ	+16.16	-7.07	-28.89	-32.32	-29.50	-43.03	-43.03			
		Success?	✓	✓	✓	✓	✓	✓	✓			
289 290 291	CircularEval	MMStar	62.02	78.38	94.14	95.96	89.90	97.98	98.99	Yes ✗		
		MMStar_C	55.96	54.95	55.56	55.76	82.63	91.92	92.73			
		Δ	-6.06	-23.43	-38.58	-40.20	-7.27	-6.06	-6.26			
		Success?	—	✓	✓	✓	✓	✗	✓			
292 293 294	Choice Confusion	MMStar	62.02	78.38	94.14	95.96	89.90	97.98	98.99	No ✓		
		MMStar_G	94.34	94.34	93.13	93.13	96.77	96.77	97.78			
		Δ	+32.32	+15.96	-1.01	-2.83	+6.87	-1.21	-1.21			
		Success?	✓	✗	✓	✓	✗	✓	✓			
295 296 297	Multi-modal Leakage	MMStar_to	22.83	27.07	28.48	28.08	44.24	51.31	52.73	Yes ✗		
		Δ	—	+4.24	+5.65	+5.25	+21.41	+28.48	+29.90			
		Success?	—	✓	✓	✓	✓	✓	✓			

Table 2: Performance of LLaVA-v1.5-7B (top) and Qwen2-VL-7B (bottom) on the MMStar dataset (Corresponding RealWorldQA results are in the Appendix 12). We compare to “Multi-modal Leakage” Chen et al. (2024a), CircularEval (Liu et al., 2024b), and “Choice Confusion” Yao et al. (2024). Clean models perform better on our perturbed dataset – confirming that the perturbed questions are indeed of equal or lower difficulty. In contrast, all contaminated models perform worse, enabling reliable detection by our method via a simple check for performance drops. “\_P” denotes the semantically perturbed version; “to” denotes text-only performance; “\_C” denotes evaluation using circular options; “\_G” denotes evaluation using choice confusion; Δ denotes the difference in performance, with positive values indicating gains. “Success?” indicates whether the method detected contamination. “Require clean model?” indicates whether the method requires access to a clean model as a baseline. If a clean model is required as reference, the method cannot be used to detect the reference models themselves, so the entry is marked as “—”. For full results, refer to Appendix E.1.

between the original and generalized versions. Clean models gain substantially on generalized benchmarks – up to +34.04 on MMStar and +21.30 on RQA – confirming their generalization ability. By contrast, contaminated variants show much smaller gains or even losses. This failure to benefit from semantically irrelevant but easier choices reflects classic memorization-based contamination. As a detection method, choice confusion meets Practicality (Req. 1) since the method detects models that perform worse on the generalized benchmark, but its sensitivity varies across fine-tuning regimes. Choice confusion fails to detect LLaVA-v1.5-7B regardless of its training strategy or the number of epochs, and for LLaVA-v1.5-7B trained with LoRA, the model shows improved performance as the number of training epochs increases. Hence the method fails to satisfy Reliability (Req. 2) while Consistency (Req. 3) is partially observed in other training strategies.

Importantly, unlike other approaches, our method requires no dataset-specific thresholds or prior knowledge of leaked data, satisfying Practicality (Req. 1). Moreover, the performance drop scales with contamination degree, satisfying Consistency (Req. 3), and persists across all training regimes—standard fine-tuning, LoRA, and full parameter unfreezing, satisfying Reliability (Req. 2).

## 324 6 ANALYSIS OF MULTI-MODAL SEMANTIC PERTURBATION

326 **Filtered images form a representative subsample.** Since manual filtering removes a substantial  
 327 portion of the original data, a natural concern is whether the filtered sets remain representative. To  
 328 test this, we first compare model performance on the full and filtered datasets and find that the results  
 329 closely align (Table 3). This confirms that the filtering step does not introduce systematic bias, and  
 330 the remaining subsets preserve the distributional properties of the original benchmarks.

331 Model	332 RQA (765 imgs)	333 RQA_filtered (440 imgs)	334 MMStar (1500 imgs)	335 MMStar_filtered (495 imgs)
332 <b>LLaVA-v1.5-7B</b>	333 49.01%	334 52.05%	335 32.87%	336 37.78%
333 <b>Qwen2-VL-7B</b>	334 70.33%	335 70.45%	336 59.80%	337 61.62%

335 Table 3: Performance of clean models on RealWorldQA (RQA) and MMStar before and after filtering.

337 **Why perturbations yield a generalized benchmark.** Our core assumption is that by preserving the  
 338 original question and only altering the answer choice, the question difficulty remains comparable,  
 339 and that clean models that answer the original question correctly will solve the variant. In addition,  
 340 we often observe that the perturbation highlights salient visual cues more clearly than the original  
 341 images (Fig. 3), collectively yielding an alternate benchmark that is similar or easier. We validate this  
 342 empirically: clean models consistently achieve higher accuracy on perturbed benchmarks (Table 2).

343 Question	344 What does the text on the traffic sign say?	345 A. Student	346 B. Children	347 C. Police
344	345	346	347	348
349	350	351	352	353



351 (a) Original



351 (b) After multi-modal semantic perturbation

352 Figure 3: Example where the perturbed variant is easier to solve than the original. In the original  
 353 image, the traffic sign is small and the text barely legible; after perturbation, the sign is enlarged and  
 354 clearly visible.

355 **Providing the question-answer pair in caption generation is critical.** As described in Sec. 4,  
 356 conditioning the caption generation on both the original question, original answer and the new answer  
 357 is critical to creating a generalized benchmark. One natural approach is to create a variant of the  
 358 original image from simply conditioning the generated caption on the question and the new correct  
 359 answer. When we evaluated clean models on images generated from this version of the prompt,  
 360 the clean model performance was much lower compared to both the original dataset and our final  
 361 perturbed dataset, with invalid perturbations appearing much more frequently, for example, due to  
 362 critical component of the image being left out so the question is ambiguous or no longer solvable.  
 363 Intuitively, the captioning model first reasons about which parts of the image need to change to make  
 364 the new answer correct, and produces a detailed caption emphasizing those changes. Flux+ControlNet  
 365 then focuses on rendering these components exactly. Finally, changing the answer is necessary to  
 366 delineate contaminated models’ behavior from simply memorizing the answer.

367 **Failure modes of multi-modal semantic perturbation.** There are cases where multi-modal perturba-  
 368 tion fails to reveal contamination. The perturbed image may differ in its visual details that it  
 369 no longer closely resembles the original. In such cases, contaminated models may answer both the  
 370 original and perturbed questions correctly as shown in Figure 4, hiding the contamination of the  
 371 model. To ensure that such failure cases are rare, we manually inspected the perturbed datasets and  
 372 verified that only 8 out of 440 images (~1.8%) from perturbed RealWorldQA and 17 out of 495  
 373 images (~3.4%) from perturbed MMStar deviate from the original question’s visual details.

374 **Limitations of multi-modal semantic perturbation framework.** For semantic perturbation to be  
 375 valid, questions must enforce visual dependence. If a question can be answered without visual input,  
 376 perturbing the image is meaningless, and altering only the answer invalidates the task. As such, we  
 377 restricted our study to RealWorldQA and MMStar, which are VQA benchmarks with strict visual  
 378 grounding. This constraint highlights an important boundary: our method is only effective when  
 379 visual semantics directly determines the correct answer.

378  
379  
380  
381  
382  
383  
384  
385  
386  
387

**Question** Which vehicle is closer to us, the school bus or the black SUV?  
 A. School bus B. Black SUV C. They are at the same distance.



(a) Original



(b) After multi-modal semantic perturbation

Figure 4: Example where a contaminated model answers both the original and perturbed questions correctly. This may occur when visual details change significantly that the perturbed image no longer closely resembles the original.

Both RealWorldQA and MMStar are multiple-choice benchmarks. Although the multiple-choice format simplifies evaluation, our framework is not inherently tied to this setting. Once visual evidence is perturbed, evaluation can be adapted to free-form tasks using string matching, likelihood-based scoring, or LLM-as-a-judge approaches. This principle extends naturally beyond multi-choice VQA.

Finally, manual filtering is required only because of current limitations of diffusion models. As generative models improve, we expect manual filtering to become unnecessary, further strengthening the scalability of our approach.

399  
400

## 7 ABLATION STUDIES

401  
402  
403  
404  
405

We next validate that the core idea—testing for memorization via *multi-modal semantic perturbations*—is robust to design choices. Specifically, we show our method is not tied to synthetic edits, scales to larger models and alternate contamination regimes, and works without GPT-4o or manual filtering.

406  
407  
408  
409  
410

**Real-world Counterfactuals: NaturalBench.** NaturalBench (Li et al., 2024) provides real counterfactual pairs – photos of the same scene under altered conditions – serving as a natural analogue to our synthetic variants. We fine-tune on one variant and evaluate its paired counterfactual with the same question. Contaminated models drop sharply (up to 45.95%), while clean models remain comparatively stable (Table 6), showing our detector generalizes beyond synthetic perturbations<sup>3</sup>. Thus, any reliable semantic variation – natural, procedural, or synthetic – fits our framework.

411  
412  
413  
414  
415  
416  
417

**Contamination with paraphrased data.** A simple but effective contamination is paraphrasing the data the model is contaminated on. To test whether models contaminated with paraphrased data can be detected, we paraphrase the questions using GPT-4o with minimal n-gram overlap. The contaminated models are then evaluated on the original benchmark and its perturbed variant. Table 4 and 5 show that contaminated models show inflated performance on original benchmarks with lowered performance on perturbed benchmarks, proving our detection method is robust against paraphrasing.

418  
419  
420  
421  
422  
423  
424  
425

Method	Epoch	RQA	RQA_P	$\Delta$
<b>Contamination with paraphrased RealWorldQA</b>				
LLaVA-v1.5-7B (clean)	—	52.05	56.36	<b>+4.31</b>
LoRA (contaminated)	1	52.03	40.00	<b>-12.03</b>
	2	55.91	40.00	<b>-15.91</b>
	3	59.09	38.86	<b>-20.23</b>
LLM+MLP (contaminated)	1	56.14	53.41	<b>-2.73</b>
	2	61.36	48.64	<b>-12.72</b>
	3	63.64	49.77	<b>-13.87</b>

426  
427  
428  
429  
430  
431

Table 4: Performance of LLaVA-v1.5-7B and contaminated variants on RealWorldQA when trained on the paraphrased benchmark. “\_P” denotes the semantically perturbed version. For full results, refer to Appendix E.5.

<sup>3</sup>Note that because counterfactuals are not guaranteed to be easier, clean-model deltas need not be positive.

Method	Epoch	MMStar	MMStar_P	$\Delta$
<b>Contamination with paraphrased MMStar</b>				
LLaVA-v1.5-7B (clean)	—	37.78	68.29	<b>+31.51</b>
LoRA (contaminated)	1	51.52	43.64	<b>-7.88</b>
	2	59.60	41.82	<b>-17.78</b>
	3	62.22	40.81	<b>-21.41</b>
LLM+MLP (contaminated)	1	47.27	46.06	<b>-1.13</b>
	2	57.60	53.54	<b>-3.06</b>
	3	62.42	57.98	<b>-4.44</b>

Table 5: Performance of LLaVA-v1.5-7B and contaminated variants on MMStar when trained on the paraphrased benchmark. “\_P” denotes the semantically perturbed version. For full results, refer to Appendix E.5.

432  
 433 **Model Scale: LLaVA-13B.** To assess scalability, we repeat the RealWorldQA experiment with  
 434 LLaVA-v1.5-13B. Table 7 shows our detector remains effective at this scale. Given that larger models  
 435 are more prone to memorization, these findings indicate the approach is suitable for stronger VLMs.

Method	Epoch	Train Set (%)	Test Set (%)	$\Delta$
Contamination with NaturalBench				
LLaVA-v1.5-7B (clean)	—	65.63	65.89	+0.26
LoRA (contaminated)	1	81.53	61.37	-20.16
	2	89.79	57.16	-32.63
	3	91.11	57.32	-33.79
LLM+MLP (contaminated)	1	79.95	58.79	-21.16
	2	97.05	54.32	-42.74
	3	98.63	53.05	-45.58

444 Table 6: Performance of clean and contaminated models  
 445 on NaturalBench. While clean model shows comparable  
 446 performance on the test set, contaminated models fail to  
 447 generalize, with performance drop upto  
 448 -45.58%. For full results, refer to Appendix E.2.

449 **Test-set leakage during Pretraining.** We simulate pretraining leakage by mixing RealWorldQA into  
 450 the 665K instruction-following pretraining corpus and training LLaVA-v1.5-7B for one epoch (Table  
 451 8). Using the same 440 filtered images, our method flags contamination, demonstrating applicability  
 452 beyond fine-tuning-only settings.

Model	RQA	RQA_P	$\Delta$
LLaVA-v1.5-7B (clean)	52.05	56.36	+4.31
Pretrain (contaminated)	51.82	50.00	-1.82

453 Table 8: Performance of clean vs. pretrained-contaminated models on RealWorldQA (440 images).

454 In addition, we test our perturbation pipeline under a more realistic contamination scenario: a mixture  
 455 of other benchmarks. We fine-tune the models with popular multi-modal benchmarks: MathVista Lu  
 456 et al. (2024b), MMMU Yue et al. (2024), MMBench Liu et al. (2024b) and CV-Bench Tong et al.  
 457 (2024), resulting in 11,280 image-question pairs, with RealWorldQA and MMStar now consisting  
 458 only of  $\sim 6.7\%$  and  $\sim 13.3\%$ , respectively. Results are in Appendix E.6 due to limited space.

459 We still observe a clean and consistent detection across all contaminated models, demonstrating  
 460 that our perturbation pipeline can reliably detect contaminated models even when the contamination  
 461 signal is weaker, which has been shown in Table 8 as well.

462 Finally, we ablate two key components of our pipeline to show modularity.

463 **Automation of filtering Process.** We replace manual validation with the  $\circ 3$  model to filter generated  
 464 image-question pairs. The automatic pass removes 471 items and retains 294, of which 253 overlap  
 465 with the manually kept set, indicating high agreement (Table 9). The exact prompt is provided in  
 466 Appendix B.

467 **Caption generation with Molmo-7B-D.** To decouple the pipeline from GPT-4o, we substitute  
 468 captioning with the lightweight open-source Molmo-7B-D Deitke et al. (2024) while keeping Flux  
 469 ControlNet for image generation. After manual filtering, this variant yields 398 valid pairs and  
 470 preserves the same detection trends, underscoring the flexibility of our approach (Table 10).

## 471 8 RELATED WORK

472 **Data Contamination in LLMs.** Brown et al. (2020) was among the first to highlight the problem  
 473 of data contamination when training models on internet-scale corpora, proposing an n-gram over-  
 474 lap-based decontamination technique that was later adopted in Bai et al. (2023). Building on this,  
 475 several detection methods exploit verbatim memorization to identify leaked test-set examples (Oren  
 476 et al., 2023; Golchin & Surdeanu, 2024; Xu et al., 2024). More specifically, Xu et al. (2024); Golchin  
 477 & Surdeanu (2024) test whether the model can accurately reconstruct masked spans of test questions,  
 478 while Oren et al. (2023) measure the log-probability of the original ordering of multiple-choice

Method	Epoch	RQA	RQA_P	$\Delta$
<b>Contamination with RealWorldQA</b>				
LLaVA-v1.5-7B (clean)	—	50.68	59.86	<b>+9.18</b>
	1	50.34	44.90	<b>-5.44</b>
LoRA (contaminated)	2	66.33	46.60	<b>-19.73</b>
	3	77.21	47.28	<b>-29.93</b>
	1	60.54	54.42	<b>-6.12</b>
LLM+MLP (contaminated)	2	63.95	55.10	<b>-8.85</b>
	3	64.63	53.40	<b>-11.23</b>

Table 9: Performance after filtering with the o3 model, resulting in 294 valid image–question pairs. Results satisfy all requirements. For full results, refer to Appendix E.3.

options. Choi et al. (2025) instead examine embedding divergence after fine-tuning, exploiting the observation that embeddings of unseen samples change more substantially than those of memorized ones. However, these methods face key limitations: Oren et al. (2023); Golchin & Surdeanu (2024); Xu et al. (2024) perform poorly on contaminated VLMs, while Choi et al. (2025) requires ground-truth clean model behavior to establish a detection threshold, reducing its practicality.

**Generalized Benchmarks for Detecting Contamination.** Yao et al. (2024) address these limitations by testing for generalization rather than memorization. They construct trivial variants of benchmark questions by replacing incorrect multiple-choice options with irrelevant answers. Contaminated models often fail on the easier variants, exposing strong memorization. However, their setup involves training for 36 epochs on a single benchmark – an unrealistic scenario for modern large-scale training. In a similar spirit, GSM-Symbolic and MATH-Perturb (Mirzadeh et al., 2024; Huang et al., 2025) introduce perturbation-based approaches, measuring performance drops on variant questions as contamination signals.

**Contamination Detection in VLMs.** VLMs differ from LLMs due to their multi-modal inputs and multi-stage alignment training, which yield distinct contamination dynamics. Lu et al. (2024a) proposed shuffling BGR color channels to mitigate spurious cues, while Song et al. (2025) introduced image masking and option shuffling to test robustness. Yet these approaches struggle to reliably detect contaminated VLMs, as observed performance drops may arise from confounding factors such as visual artifacts or biased sampling rather than true memorization. In contrast, our framework provides consistent detection across diverse fine-tuning regimes, requires no access to leaked data, and yields performance drops that correlate strongly with the degree of contamination.

## 9 CONCLUSION

Recent advances in Vision-Language Models (VLMs) have raised concerns about inflated benchmark performance due to test-set leakage from large-scale, proprietary training corpora. To overcome the limitations of existing detection methods, we introduce a novel approach based on *multi-modal semantic perturbation*. By deliberately contaminating open-source VLMs and evaluating their generalization behavior, we show that our method consistently identifies contamination where prior approaches either fail or yield inconsistent signals. These results establish multi-modal semantic perturbation as a simple and reliable framework for detecting test-set leakage in VLMs.

**Broader Impacts.** Our multi-modal semantic perturbation method aims to uncover and quantify the degree of data contamination in VLMs, promoting cleaner training pipelines and more trustworthy models. By systematically characterizing contamination behaviors, it lays the groundwork for robust model evaluation and contamination detection. While these insights could inform adversaries seeking subtler contamination schemes, we believe this work will foster the development of stronger defenses and decontamination strategies.

**Reproducibility Statement.** We will publicly release our code, models and data upon the paper’s acceptance.

**LLM Usage.** Gemini and ChatGPT were used to polish some of the paper’s writing.

540 REFERENCES  
541

542 Marah Abdin, Jyoti Aneja, Harkirat Behl, Sébastien Bubeck, Ronen Eldan, Suriya Gunasekar,  
543 Michael Harrison, Russell J. Hewett, Mojan Javaheripi, Piero Kauffmann, James R. Lee, Yin Tat  
544 Lee, Yuanzhi Li, Weishung Liu, Caio C. T. Mendes, Anh Nguyen, Eric Price, Gustavo de Rosa, Olli  
545 Saarikivi, Adil Salim, Shital Shah, Xin Wang, Rachel Ward, Yue Wu, Dingli Yu, Cyril Zhang, and  
546 Yi Zhang. Phi-4 technical report, 2024a. URL <https://arxiv.org/abs/2412.08905>.

547 Marah Abdin, Sam Ade Jacobs, Ammar Ahmad Awan, Jyoti Aneja, Ahmed Awadallah, Hany  
548 Awadalla, Nguyen Bach, Amit Bahree, Arash Bakhtiari, Harkirat Behl, et al. Phi-3 technical report:  
549 A highly capable language model locally on your phone. *arXiv preprint arXiv:2404.14219*, 2024b.  
550

551 Jinze Bai, Shuai Bai, Yunfei Chu, Zeyu Cui, Kai Dang, Xiaodong Deng, Yang Fan, Wenbin Ge,  
552 Yu Han, Fei Huang, Binyuan Hui, Luo Ji, Mei Li, Junyang Lin, Runji Lin, Dayiheng Liu, Gao Liu,  
553 Chengqiang Lu, Keming Lu, Jianxin Ma, Rui Men, Xingzhang Ren, Xuancheng Ren, Chuanqi  
554 Tan, Sinan Tan, Jianhong Tu, Peng Wang, Shijie Wang, Wei Wang, Shengguang Wu, Benfeng  
555 Xu, Jin Xu, An Yang, Hao Yang, Jian Yang, Shusheng Yang, Yang Yao, Bowen Yu, Hongyi  
556 Yuan, Zheng Yuan, Jianwei Zhang, Xingxuan Zhang, Yichang Zhang, Zhenru Zhang, Chang  
557 Zhou, Jingren Zhou, Xiaohuan Zhou, and Tianhang Zhu. Qwen technical report, 2023. URL  
558 <https://arxiv.org/abs/2309.16609>.

559 Tom B. Brown, Benjamin Mann, Nick Ryder, Melanie Subbiah, Jared Kaplan, Prafulla Dhariwal,  
560 Arvind Neelakantan, Pranav Shyam, Girish Sastry, Amanda Askell, Sandhini Agarwal, Ariel  
561 Herbert-Voss, Gretchen Krueger, Tom Henighan, Rewon Child, Aditya Ramesh, Daniel M. Ziegler,  
562 Jeffrey Wu, Clemens Winter, Christopher Hesse, Mark Chen, Eric Sigler, Mateusz Litwin, Scott  
563 Gray, Benjamin Chess, Jack Clark, Christopher Berner, Sam McCandlish, Alec Radford, Ilya  
564 Sutskever, and Dario Amodei. Language models are few-shot learners, 2020. URL <https://arxiv.org/abs/2005.14165>.  
565

566 John Canny. A computational approach to edge detection. *TPAMI*, PAMI-8(6):679–698, 1986. doi:  
567 10.1109/TPAMI.1986.4767851.  
568

569 Nicholas Carlini, Florian Tramèr, Eric Wallace, Matthew Jagielski, Ariel Herbert-Voss, Katherine  
570 Lee, Adam Roberts, Tom Brown, Dawn Song, Úlfar Erlingsson, Alina Oprea, and Colin  
571 Raffel. Extracting training data from large language models. In *30th USENIX Security Symposium (USENIX Security 21)*, pp. 2633–2650. USENIX Association, August 2021. ISBN 978-1-  
572 939133-24-3. URL <https://www.usenix.org/conference/usenixsecurity21/presentation/carlini-extracting>.  
573

574 Lin Chen, Jinsong Li, Xiaoyi Dong, Pan Zhang, Yuhang Zang, Zehui Chen, Haodong  
575 Duan, Jiaqi Wang, Yu Qiao, Dahua Lin, and Feng Zhao. Are we on the right way  
576 for evaluating large vision-language models? In A. Globerson, L. Mackey, D. Bel-  
577 grave, A. Fan, U. Paquet, J. Tomczak, and C. Zhang (eds.), *Advances in Neural In-  
578 formation Processing Systems*, volume 37, pp. 27056–27087. Curran Associates, Inc.,  
579 2024a. URL [https://proceedings.neurips.cc/paper\\_files/paper/2024/file/2f8ee6a3d766b426d2618e555b5aeb39-Paper-Conference.pdf](https://proceedings.neurips.cc/paper_files/paper/2024/file/2f8ee6a3d766b426d2618e555b5aeb39-Paper-Conference.pdf).  
580

581 Zhe Chen, Jiannan Wu, Wenhui Wang, Weijie Su, Guo Chen, Sen Xing, Muyan Zhong, Qinglong  
582 Zhang, Xizhou Zhu, Lewei Lu, Bin Li, Ping Luo, Tong Lu, Yu Qiao, and Jifeng Dai. Internvl:  
583 Scaling up vision foundation models and aligning for generic visual-linguistic tasks, 2024b. URL  
584 <https://arxiv.org/abs/2312.14238>.  
585

586 Zhe Chen, Weiyun Wang, Yue Cao, Yangzhou Liu, Zhangwei Gao, Erfei Cui, Jinguo Zhu, Shenglong  
587 Ye, Hao Tian, Zhaoyang Liu, Lixin Gu, Xuehui Wang, Qingyun Li, Yimin Ren, Zixuan Chen,  
588 Jiapeng Luo, Jiahao Wang, Tan Jiang, Bo Wang, Conghui He, Botian Shi, Xingcheng Zhang,  
589 Han Lv, Yi Wang, Wenqi Shao, Pei Chu, Zhongying Tu, Tong He, Zhiyong Wu, Huipeng Deng,  
590 Jiaye Ge, Kai Chen, Kaipeng Zhang, Limin Wang, Min Dou, Lewei Lu, Xizhou Zhu, Tong Lu,  
591 Dahua Lin, Yu Qiao, Jifeng Dai, and Wenhui Wang. Expanding performance boundaries of  
592 open-source multimodal models with model, data, and test-time scaling, 2025. URL <https://arxiv.org/abs/2412.05271>.  
593

594 Hyeong Kyu Choi, Maxim Khanov, Hongxin Wei, and Yixuan Li. How contaminated is your  
 595 benchmark? quantifying dataset leakage in large language models with kernel divergence, 2025.  
 596 URL <https://arxiv.org/abs/2502.00678>.

597 Matt Deitke, Christopher Clark, Sangho Lee, Rohun Tripathi, Yue Yang, Jae Sung Park, Moham-  
 598 madreza Salehi, Niklas Muennighoff, Kyle Lo, Luca Soldaini, Jiasen Lu, Taira Anderson, Erin  
 599 Bransom, Kiana Ehsani, Huong Ngo, YenSung Chen, Ajay Patel, Mark Yatskar, Chris Callison-  
 600 Burch, Andrew Head, Rose Hendrix, Favyen Bastani, Eli VanderBilt, Nathan Lambert, Yvonne  
 601 Chou, Arnavi Chheda, Jenna Sparks, Sam Skjonsberg, Michael Schmitz, Aaron Sarnat, Byron  
 602 Bischoff, Pete Walsh, Chris Newell, Piper Wolters, Tanmay Gupta, Kuo-Hao Zeng, Jon Borchardt,  
 603 Dirk Groeneveld, Crystal Nam, Sophie Lebrecht, Caitlin Wittlif, Carissa Schoenick, Oscar Michel,  
 604 Ranjay Krishna, Luca Weihs, Noah A. Smith, Hannaneh Hajishirzi, Ross Girshick, Ali Farhadi,  
 605 and Aniruddha Kembhavi. Molmo and pixmo: Open weights and open data for state-of-the-art  
 606 vision-language models, 2024. URL <https://arxiv.org/abs/2409.17146>.

607 Gemini Team. Gemini: A family of highly capable multimodal models, 2024.

608 Shahriar Golchin and Mihai Surdeanu. Time travel in llms: Tracing data contamination in large  
 609 language models, 2024. URL <https://arxiv.org/abs/2308.08493>.

610 Edward J. Hu, Yelong Shen, Phillip Wallis, Zeyuan Allen-Zhu, Yuanzhi Li, Shean Wang, Lu Wang,  
 611 and Weizhu Chen. Lora: Low-rank adaptation of large language models, 2021. URL <https://arxiv.org/abs/2106.09685>.

612 Kaixuan Huang, Jiacheng Guo, Zihao Li, Xiang Ji, Jiawei Ge, Wenzhe Li, Yingqing Guo, Tianle Cai,  
 613 Hui Yuan, Runzhe Wang, Yue Wu, Ming Yin, Shange Tang, Yangsibo Huang, Chi Jin, Xinyun  
 614 Chen, Chiyuan Zhang, and Mengdi Wang. Math-perturb: Benchmarking llms' math reasoning  
 615 abilities against hard perturbations, 2025. URL <https://arxiv.org/abs/2502.06453>.

616 Nikhil Kandpal, Haikang Deng, Adam Roberts, Eric Wallace, and Colin Raffel. Large language  
 617 models struggle to learn long-tail knowledge. In Andreas Krause, Emma Brunskill, Kyunghyun  
 618 Cho, Barbara Engelhardt, Sivan Sabato, and Jonathan Scarlett (eds.), *Proceedings of the 40th  
 International Conference on Machine Learning*, volume 202 of *Proceedings of Machine Learning  
 Research*, pp. 15696–15707. PMLR, 23–29 Jul 2023. URL <https://proceedings.mlr.press/v202/kandpal23a.html>.

619 Black Forest Labs. Flux. <https://github.com/black-forest-labs/flux>, 2024.

620 Baiqi Li, Zhiqiu Lin, Wenxuan Peng, Jean de Dieu Nyandwi, Daniel Jiang, Zixian Ma, Simran  
 621 Khanuja, Ranjay Krishna, Graham Neubig, and Deva Ramanan. Naturalbench: Evaluating vision-  
 622 language models on natural adversarial samples. In *The Thirty-eight Conference on Neural  
 623 Information Processing Systems Datasets and Benchmarks Track*, 2024.

624 Haotian Liu, Chunyuan Li, Yuheng Li, and Yong Jae Lee. Improved baselines with visual instruction  
 625 tuning, 2024a. URL <https://arxiv.org/abs/2310.03744>.

626 Yuan Liu, Haodong Duan, Yuanhan Zhang, Bo Li, Songyang Zhang, Wangbo Zhao, Yike Yuan, Jiaqi  
 627 Wang, Conghui He, Ziwei Liu, et al. Mmbench: Is your multi-modal model an all-around player?  
 628 In *European conference on computer vision*, pp. 216–233. Springer, 2024b.

629 Hongyuan Lu, Shujie Miao, and Wai Lam. Clean evaluations on contaminated visual language  
 630 models, 2024a. URL <https://arxiv.org/abs/2410.07030>.

631 Pan Lu, Hritik Bansal, Tony Xia, Jiacheng Liu, Chunyuan Li, Hannaneh Hajishirzi, Hao Cheng,  
 632 Kai-Wei Chang, Michel Galley, and Jianfeng Gao. Mathvista: Evaluating mathematical reasoning  
 633 of foundation models in visual contexts. In *International Conference on Learning Representations  
 (ICLR)*, 2024b.

634 Iman Mirzadeh, Keivan Alizadeh, Hooman Shahrokhi, Oncel Tuzel, Samy Bengio, and Mehrdad  
 635 Farajtabar. Gsm-symbolic: Understanding the limitations of mathematical reasoning in large  
 636 language models, 2024. URL <https://arxiv.org/abs/2410.05229>.

637 OpenAI. GPT-4o technical report. <https://openai.com/research/gpt-4o>, 2024. Ac-  
 638 cessed: 2025-05-16.

648 Yonatan Oren, Nicole Meister, Niladri Chatterji, Faisal Ladakh, and Tatsunori B. Hashimoto. Proving  
 649 test set contamination in black box language models, 2023. URL <https://arxiv.org/abs/2310.17623>.

650

651 Dingjie Song, Sicheng Lai, Shunian Chen, Lichao Sun, and Benyou Wang. Both text and images  
 652 leaked! a systematic analysis of multimodal llm data contamination, 2025. URL <https://arxiv.org/abs/2411.03823>.

653

654 Shengbang Tong, Ellis Brown, Penghao Wu, Sanghyun Woo, Manoj Middepogu, Sai Charitha Akula,  
 655 Jihan Yang, Shusheng Yang, Adithya Iyer, Xichen Pan, Austin Wang, Rob Fergus, Yann LeCun,  
 656 and Saining Xie. Cambrian-1: A fully open, vision-centric exploration of multimodal llms, 2024.

657

658 Peng Wang, Shuai Bai, Sinan Tan, Shijie Wang, Zhihao Fan, Jinze Bai, Keqin Chen, Xuejing Liu,  
 659 Jialin Wang, Wenbin Ge, Yang Fan, Kai Dang, Mengfei Du, Xuancheng Ren, Rui Men, Dayiheng  
 660 Liu, Chang Zhou, Jingren Zhou, and Junyang Lin. Qwen2-vl: Enhancing vision-language model's  
 661 perception of the world at any resolution, 2024. URL <https://arxiv.org/abs/2409.12191>.

662

663

664 xAI. Grok-1.5 vision preview. <https://x.ai/blog/grok-1.5v>, 2024.

665

666 Ruijie Xu, Zengzhi Wang, Run-Ze Fan, and Pengfei Liu. Benchmarking benchmark leakage in large  
 667 language models, 2024. URL <https://arxiv.org/abs/2404.18824>.

668

669 Feng Yao, Yufan Zhuang, Zihao Sun, Sunan Xu, Animesh Kumar, and Jingbo Shang. Data contami-  
 670 nation can cross language barriers, 2024. URL <https://arxiv.org/abs/2406.13236>.

671

672 Xiang Yue, Yuansheng Ni, Kai Zhang, Tianyu Zheng, Ruoqi Liu, Ge Zhang, Samuel Stevens, Dongfu  
 673 Jiang, Weiming Ren, Yuxuan Sun, Cong Wei, Botao Yu, Ruibin Yuan, Renliang Sun, Ming Yin,  
 674 Boyuan Zheng, Zhenzhu Yang, Yibo Liu, Wenhao Huang, Huan Sun, Yu Su, and Wenhui Chen.  
 675 Mmmu: A massive multi-discipline multimodal understanding and reasoning benchmark for expert  
 agi. In *Proceedings of CVPR*, 2024.

676

677 Chiyuan Zhang, Samy Bengio, Moritz Hardt, Benjamin Recht, and Oriol Vinyals. Understanding  
 678 deep learning requires rethinking generalization. In *International Conference on Learning  
 Representations*, 2017. URL <https://openreview.net/forum?id=Sy8gdB9xx>.

679

680 Jianrui Zhang, Mu Cai, Tengyang Xie, and Yong Jae Lee. Countercurate: Enhancing physical and  
 681 semantic visio-linguistic compositional reasoning via counterfactual examples. *Findings of the  
 Association for Computational Linguistics: ACL 2024*, 2024a.

682

683 L. Zhang, A. Rao, and M. Agrawala. Adding conditional control to text-to-image diffusion models.  
 684 2023.

685

686 Renrui Zhang, Dongzhi Jiang, Yichi Zhang, Haokun Lin, Ziyu Guo, Pengshuo Qiu, Aojun Zhou, Pan  
 687 Lu, Kai-Wei Chang, Yu Qiao, et al. Mathverse: Does our multi-modal llm truly see the diagrams  
 688 in visual math problems? In *European Conference on Computer Vision*, pp. 169–186. Springer,  
 2024b.

689

690 Yaowei Zheng, Richong Zhang, Junhao Zhang, Yanhan Ye, Zheyuan Luo, Zhangchi Feng, and  
 691 Yongqiang Ma. Llamafactory: Unified efficient fine-tuning of 100+ language models. In *Pro-  
 ceedings of the 62nd Annual Meeting of the Association for Computational Linguistics (Volume 3:  
 System Demonstrations)*, Bangkok, Thailand, 2024. Association for Computational Linguistics.  
 692 URL <http://arxiv.org/abs/2403.13372>.

693

694

695

696 APPENDIX

697

698 A EXPERIMENT SETTINGS

699

700 701 In this section, we detail all hyperparameter settings for contaminating models and for multi-modal  
 semantic perturbation of benchmarks.

702 A.1 MODEL TRAINING  
703704 We contaminate LLaVA-v1.5-7B by following the official repository <sup>4</sup> and Qwen2-VL-7B using  
705 LLaMA-Factory. All settings remain identical except for the learning rates, which were tuned over  
706 the ranges shown in Table 11.

708 709 710 711 712 713 714 715 716 717 718 719 720 721 722 723 724 725 726 727 728 729 730 731 732 733 734 735 736 737 738 739 740 741 742 743 744 745 746 747 748 749 750 751 752 753 754 755	708 709 710 711 712 713 714 715 716 717 718 719 720 721 722 723 724 725 726 727 728 729 730 731 732 733 734 735 736 737 738 739 740 741 742 743 744 745 746 747 748 749 750 751 752 753 754 755		708 709 710 711 712 713 714 715 716 717 718 719 720 721 722 723 724 725 726 727 728 729 730 731 732 733 734 735 736 737 738 739 740 741 742 743 744 745 746 747 748 749 750 751 752 753 754 755	
	708 709 710 711 712 713 714 715 716 717 718 719 720 721 722 723 724 725 726 727 728 729 730 731 732 733 734 735 736 737 738 739 740 741 742 743 744 745 746 747 748 749 750 751 752 753 754 755	708 709 710 711 712 713 714 715 716 717 718 719 720 721 722 723 724 725 726 727 728 729 730 731 732 733 734 735 736 737 738 739 740 741 742 743 744 745 746 747 748 749 750 751 752 753 754 755	708 709 710 711 712 713 714 715 716 717 718 719 720 721 722 723 724 725 726 727 728 729 730 731 732 733 734 735 736 737 738 739 740 741 742 743 744 745 746 747 748 749 750 751 752 753 754 755	708 709 710 711 712 713 714 715 716 717 718 719 720 721 722 723 724 725 726 727 728 729 730 731 732 733 734 735 736 737 738 739 740 741 742 743 744 745 746 747 748 749 750 751 752 753 754 755
Learning rate	5e-6, 1e-5, 2e-5	2e-4, 1e-4	1e-5, 2e-5, 5e-6	1e-4, 1e-3
Adapter LR	5e-6	2e-5	1e-6	1e-6
Effective batch size*	128	128	16	64
LoRA rank	—	8	—	8

715 Table 11: Hyperparameter settings for LLaVA-v1.5-7B and Qwen2-VL-7B-Instruct under standard  
716 fine-tuning and LoRA. \*Effective batch size accounts for gradient accumulation across 8 GPUs.  
717718 We perform continual fine-tuning of the model weights on 8 NVIDIA A6000 GPUs. Notice Qwen2-  
719 VL models are trained with much smaller batch sizes due to heavier GPU VRAM requirements.  
720721 A.2 MULTI-MODAL SEMANTIC PERTURBATION  
722723 Multi-modal semantic perturbation is a two-stage process. In the first process where we  
724 obtain prompts that will be provided to Flux Controlnet model is generated by using GPT-  
725 4o with api-version=2024-08-01-preview. We set temperature=0.3 and limit  
726 max\_tokens=800.727 In the second stage where we create a perturbed version of the original image based on the caption  
728 generated in the first stage, we utilize Controlnet trained with Flux diffusion model <sup>5</sup>. We follow the  
729 default hyperparameter settings in the repository, except that we enforce the generated images to have  
730 the same resolution as the original images. All images are generated with 25 steps.  
731732 A.3 COST OF MULTI-MODAL SEMANTIC PERTURBATION  
733734 First, we note that our semantic perturbation pipeline only needs to be run once to constructed the  
735 perturbed benchmark. We also note that the cost scales linearly with the size of the dataset. We list  
736 below the cost and hardware requirements of each stage of our pipeline.  
737738 **Caption Generation.** Using GPT-4o as the captioning model required on average  $\sim 75$  input tokens  
739 and  $\sim 125$  output tokens per image. This means that generating 1,000 captions would cost less  
740 than \$1.50 (USD). This stage also does not require proprietary models: it can be replaced with  
741 Molmbo-7B-D (Table 10, 22, 23), which fits on a single 24GB GPU.  
742743 **Flux+ControlNet.** Flux+ControlNet generation runs on a single 40GB GPU. With 25 sampling steps,  
744 each image takes around 15 20 seconds to generate, and this can be further reduced by decreasing the  
745 number of steps. This stage is trivially parallelizable across multiple GPUs or machines if higher  
746 throughput is needed.  
747748 **Automated Filtering with o3.** Automated filtering required on average  $\sim$  input tokens and  $\sim 200$   
749 output tokens per image. Generating 1,000 filtering decisions costs less than \$2.00 (USD).  
750751 Overall, the total cost to construct the perturbed benchmark is cheap with modest hardware require-  
752 ments. Our approach scales linearly with dataset size, making our approach practical and scalable  
753 even for reasonably large benchmarks. Finally, when real-world counterfactuals are already available  
754 as part of the benchmark design (e.g., NaturalBench in Table 6, 19), we do not need to generate  
755 perturbations at all.754 <sup>4</sup>The default training script can be found here: <https://github.com/haotian-liu/LLaVA>.  
755<sup>5</sup>Code can be accessed here: <https://github.com/XLabs-AI/x-flux>

756 **B SYSTEM PROMPTS TO GPT-4O AND o3**  
757758 To generate the semantically perturbed question, we utilize GPT-4o OpenAI (2024) and Flux diffusion  
759 model Labs (2024) trained on ControlNet Zhang et al. (2023). We generate a detailed caption about  
760 the image using GPT-4o *along with the original question, original answer and the new correct answer*  
761 with the following system prompt:  
762763 *Your job is to generate a text-to-image prompt that can be used with a diffusion model.*  
764 *Based on the question and answer, write a detailed caption so that all necessary details*  
765 *are included and the question remains solvable.*  
766 *Additionally, modify the image so that the correct answer changes. For example, if the*  
767 *question asks "How many people are in the image?", change the image to have more*  
768 *people.*769 In Section 7, we demonstrated that the manual filtering process can be automated with o3 model  
770 which is a powerful reasoning model. We utilize the following system prompt to generate model  
771 responses that can be used to filter the invalid perturbed images.  
772773 *You will be given a question and an image pair, along with the answer. Your job is to*  
774 *critically analyze the image-question pair to verify that the question can be correctly*  
775 *answered.*  
776 *In particular, ensure that one can deduce the correct answer choice and that choice only.*  
777 *If there is any ambiguity, you must reject this question. When finalizing your decision, do*  
778 *NOT take into consideration the quality of the image. As long as the question remains*  
779 *solvable, you should keep it. Provide your answer in the following format: "Answer:*  
780 *ANSWER" and answer with KEEP or REJECT.*782 **C DETECTING CONTAMINATED MODELS WITH MULTI-MODAL SEMANTIC  
783 PERTURBATION ON REALWORLDQA**  
784785 Table 12 reports results for RealWorldQA. Similar to results on MMStar, we find that (i) clean models  
786 consistently outperform contaminated ones, confirming that perturbed questions are not harder;  
787 (ii) in contrast, contaminated models show clear performance drops, enabling reliable detection  
788 without thresholds or prior knowledge (Requirement 1). The drop scales with contamination level  
789 (Requirement 3) and holds across training strategies (Requirement 2).  
790791 **D EXTENDED EVALUATION ON ADDITIONAL OPEN-SOURCE AND  
792 PROPRIETARY MODELS**  
793794 We further apply our pipeline to GPT-4o (OpenAI, 2024), Gemini-2.0-Flash (Gemini Team, 2024),  
795 Phi-3.5-V (Abdin et al., 2024b), and InternVL-2.5 (Chen et al., 2025). We do not contaminate these  
796 models. Although we cannot guarantee that these models have never encountered our evaluation  
797 data, we *assume* they are uncontaminated. Under this assumption, if our framework is sound, their  
798 performance should remain consistent across original and perturbed datasets. Indeed, our results  
799 in Table 13 confirm this expectation. Across all models, perturbed performance exceeds original  
800 performance, reinforcing that clean models generalize while contaminated ones fail. Notably, Phi-  
801 3.5-V exhibits the largest gain, while InternVL-2.5-8B remains relatively flat, demonstrating that our  
802 metric is robust across architectures. This consistency underscores the effectiveness of multi-modal  
803 semantic perturbation as a detection framework.  
804  
805806 **E FULL EXPERIMENT RESULTS**  
807808 In this section, we provide the full experiment results of multi-modal semantic perturbation across  
809 four training strategies that were omitted due to limited space.

Method	Metric	LLaVA-v1.5-7B (clean)		LoRA (contaminated)			LLM+MLP (contaminated)			(Practicality (Req. 1))
		—	—	Epoch 1	Epoch 2	Epoch 3	Epoch 1	Epoch 2	Epoch 3	
Ours	RQA	52.05	—	62.73	70.00	79.55	56.36	64.55	70.68	No ✓
	RQA_P	56.36	—	51.36	52.73	44.77	52.95	50.45	51.82	
	Δ	+4.31	—	-11.37	-17.27	-34.78	-3.41	-14.10	-18.86	
	Success?	✓	—	✓	✓	✓	✓	✓	✓	
CircularEval	RQA	52.05	—	62.73	70.00	79.55	56.36	64.55	70.68	Yes ✗
	RQA_C	36.59	—	17.95	45.23	57.50	33.18	37.05	43.40	
	Δ	-15.46	—	-44.78	-24.77	-22.05	-23.18	-27.50	-27.28	
	Success?	—	—	✓	✓	✓	✓	✓	✓	
Choice Confusion	RQA	52.05	—	62.73	70.00	79.55	56.36	64.55	70.68	No ✓
	RQA_G	66.59	—	41.36	59.09	66.14	62.95	62.50	63.64	
	Δ	+14.54	—	-21.37	-10.91	-13.41	+6.59	-2.05	-7.04	
	Success?	✓	—	✓	✓	✓	✗	✓	✓	
Multi-modal Leakage	RQA_to	34.77	—	37.27	47.05	48.41	37.73	40.68	45.00	Yes ✗
	Δ	—	—	+2.50	+12.28	+13.64	+2.96	+5.91	+10.23	
	Success?	—	—	✓	✓	✓	✓	✓	✓	
	Model	Qwen2-VL-7B (clean)		LoRA (contaminated)			LLM only (contaminated)			Require clean model?
Ours	Metric	—	—	Epoch 1	Epoch 2	Epoch 3	Epoch 1	Epoch 2	Epoch 3	(Practicality (Req. 1))
	RQA	70.45	—	79.32	87.50	88.86	74.77	78.64	85.23	No ✓
	RQA_P	71.36	—	65.00	64.55	61.59	46.82	50.45	46.59	
	Δ	+0.91	—	-14.32	-22.95	-27.27	-27.95	-28.19	-38.64	
CircularEval	Success?	✓	—	✓	✓	✓	✓	✓	✓	Yes ✗
	RQA	70.45	—	79.32	87.50	88.86	74.77	78.64	85.23	
	RQA_C	63.64	—	65.00	65.91	67.05	65.23	66.59	77.73	
	Δ	-6.81	—	-14.32	-21.59	-21.81	-9.54	-12.05	-7.50	
Choice Confusion	Success?	—	—	✓	✓	✓	✓	✓	✓	No ✓
	RQA	70.45	—	79.32	87.50	88.86	74.77	78.64	85.23	
	RQA_G	91.36	—	91.59	92.05	92.50	86.14	89.77	95.23	
	Δ	+20.91	—	+12.27	+4.55	+3.64	+11.37	+11.13	+10.00	
Multi-modal Leakage	Success?	✓	—	✗	✗	✗	✗	✗	✗	Yes ✗
	RQA_to	36.14	—	37.27	41.14	42.27	52.73	28.41	62.50	
	Δ	—	—	+1.13	+5.00	+6.13	+16.59	-7.73	+26.36	
	Success?	—	—	✓	✓	✓	✓	✗	✓	

Table 12: Performance of LLaVA-v1.5-7B (top) and Qwen2-VL-7B (bottom) on the RealWorldQA dataset. We compare to “Multi-modal Leakage” Chen et al. (2024a), CircularEval (Liu et al., 2024b), and “Choice Confusion” Yao et al. (2024). Clean models perform better – confirming that the perturbed questions are indeed of equal or lower difficulty. In contrast, all contaminated models perform worse, enabling reliable detection by our method via a simple check for performance drops. RQA denotes RealWorldQA and “\_P” denotes the semantically perturbed version; “to” denotes text-only performance; “\_C” denotes evaluation using circular options; “\_G” denotes evaluation using choice confusion;  $\Delta$  denotes the difference in performance, with positive values indicating gains. “Success?” indicates whether the method detected contamination. “Require clean model?” indicates whether the method requires access to a clean model as a baseline. If a clean model is required as reference, the method cannot be used to detect the reference models themselves, so the entry is marked as “—”. For full results, refer to Appendix E.1.

Model	RQA	RQA_P	$\Delta$
Gemini-2.0-Flash	68.37	71.59	+3.22
GPT-4o	65.68	69.93	+4.25
Phi3.5-Vision	52.68	68.86	+16.18
InternVL-2.5-8B	64.05	64.77	+0.72

Table 13: Accuracy on the original vs. perturbed datasets for open-source and proprietary models.  $\Delta$  indicates the accuracy change.

## E.1 FULL RESULTS ON LLaVA-v1.5-7B AND QWEN2-VL-7B

Table 14, 15, 16, and 17 list out all results for four varying training strategies for LLaVA-v1.5-7B and Qwen2-VL-7B, including the non-default training strategies for each model which were omitted due to limited space. Note that the results here are computed on 440 manually filtered images. Our approach detects contaminated models regardless of the training strategies and satisfies all three requirements.

Model	Epoch	RQA (%)	RQA_P (%)	$\Delta$
<b>LLaVA-v1.5-7B</b>	—	52.05	56.36	<b>+4.31</b>
<b>Contamination with RealWorldQA</b>				
<b>LoRA</b>	1	62.73	51.36	<b>-11.37</b>
	2	70.00	52.73	<b>-17.27</b>
	3	79.55	44.77	<b>-34.78</b>
<b>LLM only</b>	1	58.41	51.59	<b>-6.82</b>
	2	63.64	50.68	<b>-12.96</b>
	3	70.91	47.05	<b>-23.86</b>
<b>LLM+MLP</b>	1	56.36	52.95	<b>-3.41</b>
	2	64.55	50.45	<b>-14.10</b>
	3	70.68	51.82	<b>-18.86</b>
<b>ALL</b>	1	56.36	54.32	<b>-2.04</b>
	2	64.77	52.73	<b>-12.04</b>
	3	70.23	52.05	<b>-18.18</b>

Table 14: Performance of clean and contaminated LLaVA-v1.5-7B models on RealWorldQA. “\_P” denotes the semantically perturbed version. All three requirements are satisfied.

Model	Epoch	RQA (%)	RQA_P (%)	$\Delta$
<b>LLaVA-v1.5-7B</b>	—	37.78	69.29	<b>+31.51</b>
<b>Contamination with MMStar</b>				
<b>LoRA</b>	1	52.53	44.24	<b>-8.29</b>
	2	50.71	37.58	<b>-13.13</b>
	3	54.34	38.18	<b>-16.16</b>
<b>LLM only</b>	1	44.85	37.98	<b>-6.87</b>
	2	48.48	38.99	<b>-9.49</b>
	3	55.15	38.59	<b>-16.56</b>
<b>LLM+MLP</b>	1	39.39	32.12	<b>-7.27</b>
	2	49.70	38.38	<b>-11.32</b>
	3	53.54	38.99	<b>-14.55</b>
<b>ALL</b>	1	41.82	33.33	<b>-8.49</b>
	2	48.89	37.37	<b>-11.52</b>
	3	50.71	36.97	<b>-13.74</b>

Table 16: Performance of clean and contaminated LLaVA-v1.5-7B models on MMStar. “\_P” denotes the semantically perturbed version. All three requirements are satisfied.

Model	Epoch	RQA (%)	RQA_P (%)	$\Delta$
<b>Qwen2-VL-7B</b>	—	70.45	71.36	<b>+0.91</b>
<b>Contamination with RealWorldQA</b>				
<b>LoRA</b>	1	79.32	65.00	<b>-14.32</b>
	2	87.50	64.55	<b>-22.95</b>
	3	88.86	61.59	<b>-27.27</b>
<b>LLM only</b>	1	74.77	46.82	<b>-27.95</b>
	2	78.64	50.45	<b>-28.19</b>
	3	85.23	46.59	<b>-38.64</b>
<b>LLM+MLP</b>	1	75.23	57.95	<b>-17.28</b>
	2	88.18	49.77	<b>-38.41</b>
	3	93.18	47.50	<b>-45.68</b>
<b>ALL</b>	1	74.77	39.09	<b>-35.68</b>
	2	78.18	45.91	<b>-32.27</b>
	3	87.50	40.45	<b>-47.05</b>

Table 15: Performance of clean and contaminated Qwen2-VL-7B models on RealWorldQA. “\_P” denotes the semantically perturbed version. All three requirements are satisfied.

Method	Epoch	RQA (%)	RQA_P (%)	$\Delta$
<b>Qwen2-VL-7B</b>	—	62.02	78.18	<b>+16.16</b>
<b>Contamination with MMStar</b>				
<b>LoRA</b>	1	77.37	73.33	<b>-4.04</b>
	2	87.88	68.48	<b>-19.40</b>
	3	91.52	67.47	<b>-24.05</b>
<b>LLM only</b>	1	80.20	50.71	<b>-29.49</b>
	2	94.95	52.32	<b>-42.63</b>
	3	97.17	49.09	<b>-48.08</b>
<b>LLM+MLP</b>	1	83.43	55.96	<b>-27.47</b>
	2	94.95	52.93	<b>-42.02</b>
	3	97.98	51.11	<b>-46.87</b>
<b>ALL</b>	1	71.31	47.27	<b>-24.04</b>
	2	93.13	43.64	<b>-49.49</b>
	3	96.77	44.04	<b>-52.73</b>

Table 17: Performance of clean and contaminated Qwen2-VL-7B models on MMStar. “\_P” denotes the semantically perturbed version. All three requirements are satisfied.

## E.2 FULL RESULTS WITH LLAVA-v1.5-13B AND NATURALBENCH

Table 18 lists full results for LLaVA-v1.5-13B model trained on RealWorldQA. Note that the results here are computed on 440 manually filtered images. Table 19 lists full results for LLaVA-v1.5-7B trained on one variant of NaturalBench and tested on the counterfactual version. The clean and consistent detection of contaminated models show that our approach can be applied to models of larger scale and to real-world perturbations.

## E.3 FULL RESULTS WITH $\circ 3$ FILTERING

Table 20 and 21 list out all results for contamination detection results after filtering the perturbed images with  $\circ 3$  model. To clarify, filtering with  $\circ 3$  model results in 294 images. Our approach still detects contaminated models and satisfies all three requirements, proving that our pipeline design is modular and can be automated.

Model	Epoch	RQA (%)	RQA_P (%)	$\Delta$
<b>LLaVA-v1.5-13B</b>	—	51.14	57.27	<b>+6.13</b>
<b>Contamination with RealWorldQA</b>				
<b>LoRA</b>	1	74.32	38.18	<b>-36.14</b>
	2	73.18	32.73	<b>-40.45</b>
	3	77.05	34.77	<b>-42.28</b>
<b>LLM only</b>	1	57.05	44.77	<b>-12.28</b>
	2	68.18	44.32	<b>-23.86</b>
	3	68.64	43.86	<b>-24.78</b>
<b>LLM+MLP</b>	1	56.59	37.50	<b>-19.09</b>
	2	71.59	38.86	<b>-32.73</b>
	3	75.45	37.27	<b>-38.18</b>
<b>ALL</b>	1	57.73	44.55	<b>-13.18</b>
	2	68.41	44.32	<b>-24.09</b>
	3	69.09	43.41	<b>-25.68</b>

Table 18: Performance of LLaVA-v1.5-13B models on the RealWorldQA benchmark and its semantically perturbed version consisting of 440 image-question pairs. All three requirements are satisfied.

Model	Epoch	Train (%)	Test (%)	$\Delta$
<b>LLaVA-v1.5-7B</b>	—	65.63	65.89	<b>+0.26</b>
<b>Contamination with NaturalBench</b>				
<b>LoRA</b>	1	81.53	61.37	<b>-20.16</b>
	2	89.79	57.16	<b>-32.63</b>
	3	91.11	57.32	<b>-33.79</b>
<b>LLM only</b>	1	77.63	61.95	<b>-15.68</b>
	2	88.11	57.89	<b>-30.21</b>
	3	90.58	57.32	<b>-33.26</b>
<b>LLM+MLP</b>	1	79.95	58.79	<b>-21.16</b>
	2	97.05	54.32	<b>-42.74</b>
	3	98.63	53.05	<b>-45.58</b>
<b>ALL</b>	1	81.84	58.42	<b>-23.42</b>
	2	97.05	54.47	<b>-42.58</b>
	3	98.63	52.68	<b>-45.95</b>

Table 19: Performance of clean and contaminated LLaVA-v1.5-7B models on NaturalBench. Test set denotes a natural counterfactual version of the train set. Clean model maintains a similar performance while contaminated models drop in performance for upto -45.95%.

Model	Epoch	RQA (%)	RQA_P (%)	$\Delta$
<b>Contamination with RealWorldQA</b>				
<b>LLaVA (clean)</b>	—	50.68	59.86	<b>+9.18</b>
<b>LoRA (contaminated)</b>	1	50.34	44.90	<b>-5.44</b>
	2	66.33	46.60	<b>-19.73</b>
	3	77.21	47.28	<b>-29.93</b>
<b>LLM (contaminated)</b>	1	59.86	56.80	<b>-3.06</b>
	2	63.95	55.10	<b>-8.85</b>
	3	68.71	50.00	<b>-18.71</b>
<b>LLM+MLP (contaminated)</b>	1	58.50	54.42	<b>-4.08</b>
	2	60.54	54.42	<b>-6.12</b>
	3	64.97	53.40	<b>-11.57</b>
<b>ALL (contaminated)</b>	1	59.86	56.46	<b>-3.40</b>
	2	64.63	53.40	<b>-11.23</b>
	3	69.05	50.34	<b>-18.71</b>

Table 20: Performance of clean and contaminated LLaVA-v1.5-7B models on RealWorldQA. “\_P” denotes the semantically perturbed version. Note that accuracies are measured on 294 filtered images. All three requirements are satisfied.

Model	Epoch	RQA (%)	RQA_P (%)	$\Delta$
<b>Contamination with RealWorldQA</b>				
<b>Qwen2-VL (clean)</b>	—	74.15	74.83	<b>+0.68</b>
<b>LoRA (contaminated)</b>	1	77.21	74.83	<b>-2.38</b>
	2	78.91	74.15	<b>-4.76</b>
	3	79.59	74.15	<b>-5.44</b>
<b>LLM (contaminated)</b>	1	79.25	56.12	<b>-23.13</b>
	2	85.37	54.42	<b>-30.95</b>
	3	90.48	55.44	<b>-35.04</b>
<b>LLM+MLP (contaminated)</b>	1	77.89	62.24	<b>-15.65</b>
	2	87.41	57.48	<b>-29.93</b>
	3	88.78	58.16	<b>-30.62</b>
<b>ALL (contaminated)</b>	1	80.27	58.50	<b>-21.77</b>
	2	90.82	53.40	<b>-37.42</b>
	3	92.52	52.04	<b>-40.48</b>

Table 21: Performance of clean and contaminated Qwen2-VL-7B models on RealWorldQA. “\_P” denotes the semantically perturbed version. Note that accuracies are measured on 294 filtered images. All three requirements are satisfied.

#### E.4 FULL RESULTS WITH MOLMO-7B-D AS CAPTIONING MODEL

Table 22 and 23 list full results for LLaVA-v1.5-7B and Qwen2-VL-7B models evaluated on perturbed images generated from Molmo-7B-D captions. Note that this pipeline yields 398 valid image-question pairs after manual filtering. Both results show clean detection trends, satisfying all three requirements.

#### E.5 FULL RESULTS WITH CONTAMINATION WITH PARAPHRASED DATA

Table 24 and 25 list full results for LLaVA-v1.5-7B and Qwen2-VL-7B models on RealWorldQA and table 26 and 27 on MMStar. To clarify, the models are trained with a paraphrased version of the original benchmark, and are evaluated on the original benchmark.

972	Model	Config	RQA (%)	RQA_P (%)	$\Delta$ (%)
Contamination with RealWorldQA					
974	LLaVA (clean)	—	44.22	52.01	<b>+7.79</b>
975	LoRA (contaminated)	1	44.97	35.93	<b>-9.04</b>
976		2	55.78	32.66	<b>-23.12</b>
977		3	70.35	32.91	<b>-37.44</b>
978	LLM (contaminated)	1	52.76	41.96	<b>-10.80</b>
979		2	53.02	43.97	<b>-9.05</b>
980		3	53.52	43.72	<b>-9.80</b>
981	LLM+MLP (contaminated)	1	56.53	39.95	<b>-16.58</b>
982		2	60.80	39.45	<b>-21.35</b>
983		3	61.56	39.95	<b>-21.61</b>
984	ALL (contaminated)	1	62.81	35.43	<b>-27.38</b>
985		2	61.81	35.93	<b>-25.88</b>
986		3	62.56	35.68	<b>-26.88</b>

Table 22: Performance of clean and contaminated LLaVA-v1.5-7B models on RealWorldQA. “\_P” denotes the semantically perturbed version. Note that accuracies are measured on 398 filtered images. All three requirements are satisfied.

More concretely, we prompt GPT-4o to generate three possible paraphrases of the original question, and select the one with the lowest 5-gram overlap with the original question, enforcing the model to use different sentence structures and vocabularies.

Furthermore, we observe that models contaminated on the paraphrased version of the questions show inflated performance on the original benchmark, validating our paraphrasing pipeline. The clean and consistent detection proves that our perturbation pipeline is robust against paraphrasing, which is a challenging setting for contamination detection.

997	Model	Epoch	RQA (%)	RQA_P (%)	$\Delta$
Contamination with paraphrased RealWorldQA					
999	LLaVA (clean)	—	52.05	56.36	<b>+4.31</b>
1000	LoRA (contaminated)	1	52.03	40.00	<b>-12.03</b>
1001		2	55.91	40.00	<b>-15.91</b>
1002		3	59.09	38.86	<b>-20.23</b>
1003	LLM (contaminated)	1	56.14	54.09	<b>-2.05</b>
1004		2	60.91	49.09	<b>-11.82</b>
1005		3	63.64	50.45	<b>-13.19</b>
1006	LLM+MLP (contaminated)	1	56.14	53.41	<b>-2.73</b>
1007		2	61.36	48.64	<b>-12.72</b>
1008		3	63.64	49.77	<b>-13.87</b>
1009	ALL (contaminated)	1	55.91	53.64	<b>-2.27</b>
1010		2	62.05	48.86	<b>-13.19</b>
1011		3	63.86	50.00	<b>-13.86</b>

Table 24: Performance of clean and contaminated LLaVA-v1.5-7B models on RealWorldQA. “\_P” denotes the semantically perturbed version. Note that the models are trained with paraphrased version of the original benchmark. All three requirements are satisfied.

Model	Config	RQA (%)	RQA_P (%)	$\Delta$ (%)
Contamination with RealWorldQA				
Qwen2-VL (clean)	—	61.81	65.08	<b>+3.27</b>
LoRA (contaminated)	1	63.57	59.05	<b>-4.52</b>
	2	67.84	52.26	<b>-15.58</b>
	3	68.84	52.26	<b>-16.58</b>
LLM (contaminated)	1	78.14	40.70	<b>-37.44</b>
	2	84.67	32.16	<b>-52.51</b>
	3	87.19	35.43	<b>-51.76</b>
LLM+MLP (contaminated)	1	73.12	45.48	<b>-27.64</b>
	2	83.42	34.67	<b>-48.75</b>
	3	85.18	35.93	<b>-49.25</b>
ALL (contaminated)	1	76.38	39.95	<b>-36.43</b>
	2	88.94	32.41	<b>-56.53</b>
	3	90.20	31.41	<b>-58.79</b>

Table 23: Performance of clean and contaminated Qwen2-VL-7B models on RealWorldQA. “\_P” denotes the semantically perturbed version. Note that accuracies are measured on 398 filtered images. All three requirements are satisfied.

Model	Epoch	RQA (%)	RQA_P (%)	$\Delta$
Contamination with paraphrased RealWorldQA				
Qwen2-VL (clean)	—	70.45	71.59	<b>+1.14</b>
LoRA (contaminated)	1	72.50	71.59	<b>-0.91</b>
	2	73.86	69.55	<b>-4.31</b>
	3	75.23	69.32	<b>-5.91</b>
LLM (contaminated)	1	78.41	53.86	<b>-24.55</b>
	2	87.05	56.59	<b>-30.46</b>
	3	89.55	54.32	<b>-35.23</b>
LLM+MLP (contaminated)	1	80.00	52.50	<b>-27.50</b>
	2	87.05	56.59	<b>-30.46</b>
	3	88.64	55.23	<b>-33.41</b>
ALL (contaminated)	1	75.45	51.82	<b>-23.63</b>
	2	86.36	56.36	<b>-30.00</b>
	3	90.23	55.45	<b>-34.78</b>

Table 25: Performance of clean and contaminated Qwen2-VL-7B models on RealWorldQA. “\_P” denotes the semantically perturbed version. Note that the models are trained with paraphrased version of the original benchmark. All three requirements are satisfied.

1015  
1016  
1017  
1018  
1019  
1020  
1021  
1022  
1023  
1024  
1025

Model	Epoch	MMStar (%)	MMStar_P (%)	$\Delta$
Contamination with paraphrased MMStar				
LLaVA (clean)	—	37.78	68.29	+31.51
LoRA (contaminated)	1	51.52	43.64	-7.88
	2	59.60	41.82	-17.78
	3	62.22	40.81	-21.41
LLM (contaminated)	1	47.47	45.68	-1.79
	2	53.13	50.39	-2.74
	3	61.82	53.37	-8.45
LLM+MLP (contaminated)	1	47.27	46.06	-1.13
	2	57.60	53.54	-3.06
	3	62.42	57.98	-4.44
ALL (contaminated)	1	46.87	45.25	-1.62
	2	53.33	49.52	-3.81
	3	62.42	57.58	-4.84

Table 26: Performance of clean and contaminated LLaVA-v1.5-7B models on MMStar. “\_P” denotes the semantically perturbed version. Note that the models are trained with paraphrased version of the original benchmark. All three requirements are satisfied.

Model	Epoch	MMStar (%)	MMStar_P (%)	$\Delta$
Contamination with paraphrased MMStar				
Qwen2-VL (clean)	—	62.02	78.18	+16.16
LoRA (contaminated)	1	78.87	67.48	-11.39
	2	83.33	64.95	-18.38
	3	85.70	63.74	-21.96
LLM (contaminated)	1	89.09	60.61	-28.48
	2	96.36	55.76	-40.60
	3	97.98	54.34	-43.64
LLM+MLP (contaminated)	1	87.27	61.62	-25.65
	2	97.17	55.96	-41.21
	3	97.78	56.36	-41.42
ALL (contaminated)	1	80.20	63.64	-16.56
	2	94.95	54.95	-40.00
	3	96.77	55.15	-41.62

Table 27: Performance of clean and contaminated Qwen2-VL-7B models on MMStar. “\_P” denotes the semantically perturbed version. Note that the models are trained with paraphrased version of the original benchmark. All three requirements are satisfied.

## E.6 FULL RESULTS WITH CONTAMINATION WITH A MIXTURE OF DATASETS

Table 28 and 29 list full results for LLaVA-v1.5-7B and Qwen2-VL-7B models on RealWorldQA and table 30 and 31 on MMStar. All models have been fine-tuned on a mixture of 6 popular multi-modal benchmarks: MathVista Lu et al. (2024b), MMBench Liu et al. (2024b), MMMU Yue et al. (2024), CV-Bench Tong et al. (2024), MMStar and RealWorldQA, resulting in 11,280 image-question pairs. We test whether our approach can still detect contamination on RealWorldQA and MMStar, which now consist only of ~6.7% and ~13.3% of the fine-tuning dataset, respectively. All four tables show clean and consistent detection results, satisfying all three requirements.

Model	Epoch	RQA (%)	RQA_P (%)	$\Delta$
Contamination with mixture of 6 benchmarks				
LLaVA (clean)	—	52.05	56.36	+4.31
LoRA (contaminated)	1	45.91	41.59	-4.32
	2	62.73	40.23	-22.50
	3	75.45	42.05	-33.40
LLM (contaminated)	1	59.55	52.27	-7.28
	2	65.68	50.23	-15.45
	3	67.05	46.14	-20.91
LLM+MLP (contaminated)	1	57.95	52.05	-5.90
	2	61.14	50.91	-10.23
	3	64.32	48.86	-15.46
ALL (contaminated)	1	60.00	51.82	-8.18
	2	65.91	48.86	-17.05
	3	67.95	46.82	-21.13

Table 28: Performance of clean and contaminated LLaVA-v1.5-7B models on RealWorldQA. “\_P” denotes the semantically perturbed version. All models are contaminated with a mixture of 6 benchmarks, resulting in 11,280 image-question pairs.

Model	Epoch	RQA (%)	RQA_P (%)	$\Delta$
Contamination with mixture of 6 benchmarks				
Qwen2-VL (clean)	—	70.45	71.36	+0.91
LoRA (contaminated)	1	72.95	70.00	-2.95
	2	75.91	68.18	-7.73
	3	76.14	68.31	-7.83
LLM (contaminated)	1	77.50	50.00	-27.50
	2	85.00	45.68	-39.32
	3	88.18	47.95	-40.23
LLM+MLP (contaminated)	1	75.45	53.41	-22.04
	2	85.45	48.18	-37.27
	3	86.36	47.50	-38.86
ALL (contaminated)	1	78.64	50.00	-28.64
	2	87.73	46.59	-41.14
	3	89.32	46.59	-42.73

Table 29: Performance of clean and contaminated Qwen2-VL-7B models on RealWorldQA. “\_P” denotes the semantically perturbed version. All models are contaminated with a mixture of 6 benchmarks, resulting in 11,280 image-question pairs.

1080	Model	Epoch	MMStar (%)	MMStar_P (%)	Δ
Contamination with mixture of 6 benchmarks					
1082	LLaVA (clean)	—	37.78	68.29	+31.51
1083	LoRA (contaminated)	1	45.86	26.67	-19.19
1084		2	83.43	54.14	-29.29
1085		3	85.25	52.93	-32.32
1086	LLM (contaminated)	1	42.73	38.28	-4.45
1087		2	62.02	35.15	-26.87
1088		3	73.54	41.82	-31.72
1089	LLM+MLP (contaminated)	1	34.65	33.03	-1.62
1090		2	62.42	38.59	-23.83
		3	82.22	48.48	-33.74
1091	ALL (contaminated)	1	32.22	30.41	-1.81
1092		2	77.78	45.05	-32.73
1093		3	81.82	45.45	-36.37

Table 30: Performance of clean and contaminated LLaVA-v1.5-7B models on MMStar. “\_P” denotes the semantically perturbed version. All models are contaminated with a mixture of 6 benchmarks, resulting in 11,280 image-question pairs.

Model	Epoch	MMStar (%)	MMStar_P (%)	Δ
Contamination with mixture of 6 benchmarks				
Qwen2-VL (clean)	—	62.02	78.18	+16.16
LoRA (contaminated)	1	78.38	71.31	-7.07
	2	94.14	65.25	-28.89
	3	95.96	63.64	-32.32
LLM (contaminated)	1	89.90	60.40	-29.50
	2	97.98	54.95	-43.03
	3	98.99	55.96	-43.03
LLM+MLP (contaminated)	1	90.10	61.41	-28.69
	2	97.17	55.56	-41.61
	3	98.79	55.96	-42.83
ALL (contaminated)	1	85.86	62.83	-23.03
	2	89.70	57.37	-32.33
	3	93.74	55.76	-37.98

Table 31: Performance of clean and contaminated Qwen2-VL-7B models on RealWorldQA. “\_P” denotes the semantically perturbed version. All models are contaminated with a mixture of 6 benchmarks, resulting in 11,280 image-question pairs.

## E.7 FULL RESULTS WITH CONTAMINATION IN FREE-FORM QA TASK

To verify that our perturbation pipeline extends beyond multiple-choice VQA tasks, we use CounterCurate Zhang et al. (2024a), which consists of synthetically generated counterfactual images designed to test compositional knowledge. More concretely, CounterCurate contains a subset of images that are generated from DALLE-3 with prompts that only differ in the attributes or noun (e.g. “A woman with blue hat” vs. “A man with red hat”). Hence both images remain relatively consistent, semantically and spatially.

While CounterCurate is originally a multiple-choice VQA benchmark, the answer options are natural sentences, making it suitable for testing model’s free-form QA. We reformulate the task into a captioning setup: we ask the model to generate an overview description of the image focusing on the main entity and treat the correct choice as the ground-truth caption. We then use GPT-4o as a judge to decide whether the model’s description is closer to the ground-truth caption or to the caption of the counterfactual image.

Concretely, we randomly sample 500 image-question pairs from the dataset and use the corresponding 500 counterfactuals as the perturbed test set. In this setting we cannot expect the clean model to perform better on the counterfactual set as the counterfactuals need not be easier than the original; instead, we look at how the performance gap between original vs. counterfactual changes under contamination.

Since we are testing the models on a free-form language generation task with an unlimited output space, evaluated by an LLM-as-a-judge rather than exact matching over a fixed set of options, the contamination signal can be weaker. As a result, we see some failure cases for models trained for 1 epoch, with standard fine-tuning. However, our pipeline still detects all other contaminated models and contaminated models show a larger performance degradation between the original and counterfactual sets than the clean model, indicating that the core principle of our pipeline extends to free-form setup beyond multiple-choice VQA.

1134  
 1135  
 1136  
 1137  
 1138  
 1139  
 1140  
 1141  
 1142  
 1143  
 1144  
 1145  
 1146  
 1147  
 1148  
 1149  
 1150  
 1151  
 1152  
 1153  
 1154  
 1155  
 1156  
 1157  
 1158  
 1159  
 1160  
 1161  
 1162  
 1163

Model	Epoch	Train (%)	Test (%)	$\Delta$
<b>LLaVA</b>	—	72.20	76.87	<b>+4.68</b>
<b>LoRA</b>	1	89.44	88.65	<b>-0.79</b>
	2	89.66	88.44	<b>-1.22</b>
	3	90.30	87.79	<b>-2.51</b>
<b>LLM</b>	1	87.72	88.87	<b>+1.15</b>
	2	88.79	86.72	<b>-2.07</b>
	3	90.73	86.94	<b>-3.79</b>
<b>LLM+MLP</b>	1	87.72	88.01	<b>+0.29</b>
	2	89.44	86.08	<b>-3.36</b>
	3	89.87	85.84	<b>-4.03</b>
<b>ALL</b>	1	87.72	88.87	<b>+1.15</b>
	2	90.09	86.94	<b>-3.15</b>
	3	90.30	85.87	<b>-4.43</b>

1164 Table 32: Performance of clean and contaminated models on the training and test splits of CounterCu-  
 1165 rate. The train set denotes a free-form QA task generated from a random sample of 500 image-caption  
 1166 pairs, and the test set denotes the counterfactuals. Red color denotes cases where our method will fail  
 1167 to detect contamination. Accuracies are measured with an LLM-as-a-judge. Since this is a free-form  
 1168 language generation task, contamination signals are weaker, leading to some detection failures under  
 1169 light contamination (standard fine-tuning for 1 epoch with LLM, LLM+MLP, ALL), while these  
 1170 settings become detectable when contamination is stronger. Across all configurations, contaminated  
 1171 models still show a larger degradation between the original and counterfactual sets than the clean  
 1172 model, indicating that the core principle of our pipeline extends to the free-form setup.  
 1173  
 1174  
 1175  
 1176  
 1177  
 1178  
 1179  
 1180  
 1181  
 1182  
 1183  
 1184  
 1185  
 1186  
 1187